Tetrahedron: *Asymmetry* 20 (2009) 1778–1790

Contents lists available at ScienceDirect

Tetrahedron: *Asymmetry*

journal homepage: www.elsevier.com/locate/tetasy

Chiraloptical properties of adducts derived from cyclic nitrones and 2(*5H*)-furanones. Combined experimental and theoretical studies

Sebastian Stecko, Jadwiga Frelek, Marek Chmielewski *

Institute of Organic Chemistry, Polish Academy of Sciences, Kasprzaka 44/52, 01-224 Warsaw, Poland

ARTICLE INFO

Article history:
Received 21 May 2009
Accepted 25 June 2009
Available online 17 July 2009

ABSTRACT

The validity of the Bucourt–Legrand empirical rule, which relates the configuration at the α-carbon atom in the lactone unit with the sign of the lactone n→π* transition observed in the electronic circular dichroism (ECD) spectrum of 5-5-5 and 5-5-6 fused heterocyclic systems, was investigated. For this purpose, a combination of ECD spectroscopy, time-dependent density functional theory (TD-DFT) and molecular modelling calculations supported additionally by X-ray diffraction analysis, was applied. Model compounds were obtained via the 1,3-dipolar cycloaddition of 2(*5H*)-furanones and five- and six-membered cyclic nitrones. In addition, cycloadducts either with or without an additional interfering chromophore were selected. A comparison of the recorded ECD spectra with those simulated by the TD-DFT calculations gave a reasonable interpretation of the excitations observed in the 210–230 nm spectroscopic range. Generally, calculations confirmed the validity of the Bucourt–Legrand rule and demonstrated that ECD may be used as a highly sensitive probe for the three-dimensional molecular structure of the systems studied herein. Notable behaviour, however, was observed in the case of some 5-5-6 fused systems substituted with BnO group. In these cases, the conformational liability and coupling of molecular lactone excitation with other chromophores cause a change of orientation of the transition dipole moments resulting in a breakdown of the rule.

1. Introduction

The 1,3-dipolar cycloaddition (1,3-DC) reactions represent a powerful tool for the construction of both heterocyclic and carbocyclic rings.[1] The best-known processes of this kind are reactions between nitrones and alkenes leading to the formation of isoxazolidine rings.[1] The efficient formation of functionalized isoxazolidines and, after subsequent hydrogenolysis of N-O bond, also of the β-amino alcohols enables the facile syntheses of various nitrogen-containing compounds.[2–7] The utility of 1,3-DC involving nitrones in the synthesis of iminosugars has been demonstrated by numerous research groups,[8–11] including our own.[12]

Recently, we have demonstrated a general approach to iminosugars via the cycloaddition reaction between cyclic nitrones **1–2** and five- or six-membered unsaturated lactones **3–6** as a key step in the synthesis (Chart 1).[12] These efforts were preceded by the detailed studies on the asymmetric induction observed during reactions between cyclic nitrones (e.g., **1** and **2**) and both types of lactones (e.g., **3–6**)[13,14] supported by DFT and molecular modelling calculations.[15]

A direct assignment of the absolute configuration of type **A** and type **B** cycloadducts (Scheme 1) is not straightforward. The standard NMR techniques often do not provide unequivocal results because of the overlap of diagnostic resonances with others. Moreover, adducts frequently do not form crystals suitable for X-ray analysis. These difficulties prompted us to undertake the investigation of electronic circular dichroism spectroscopy to find the relationship between the stereostructure of a cycloadduct and its respective CD data.

In 1967, Legrand and Bucourt[16] established a general rule for five-, six- and seven-membered lactones, which correlates the sign of the n→π* Cotton effect (CE) with the sign of the O–C(=O)–C_α–C_β dihedral angle, called the '*ring-chirality rule*'. According to this rule, a negative n→π* CE is expected for a positive dihedral angle and a positive CE is expected for a negative angle. This rule, however, is only valid for the planar lactone chromophoric system.

Previously, we have shown that circular dichroism spectroscopy is a useful tool for the determination of the absolute configuration at the newly formed stereogenic centres of cycloadducts obtained via 1,3-DC reactions between cyclic nitrones and δ-lactones.[13a,b] These studies pointed out that the ring-chirality rule can be successfully applied in the stereochemical analysis of cycloadducts derived from six-membered lactones, for example, **4** and **5**, and cyclic nitrones **1** and **2**. These studies revealed that a negative sign of the n→π* CE at around 220–230 nm corresponds to an (*R*)-absolute configuration at the α-carbon atom whereas the (*S*)-configurations at that atom corresponds to an opposite sign of this transition.

* Corresponding author. Tel./fax: +48 22 632 66 81.
E-mail address: chmiel@icho.edu.pl (M. Chmielewski).

0957-4166/$ - see front matter © 2009 Elsevier Ltd. All rights reserved.
doi:10.1016/j.tetasy.2009.06.017

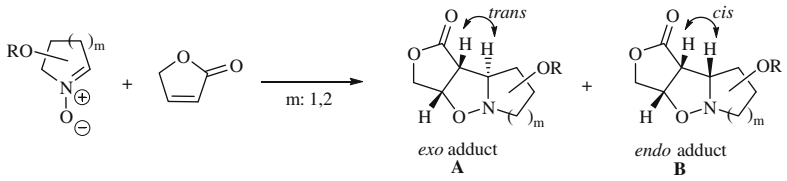

Scheme 1.

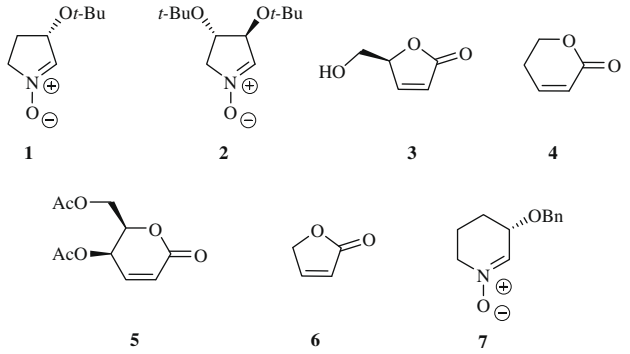

Chart 1.

Moreover, it was demonstrated that both the substitution of the lactone ring and its conformation influence the shape of the CD spectra.

Herein, we report our extended studies in this area concerning the chiraloptical properties of cycloadducts derived from the five-membered nitrones (e.g., **1** and **2**) and 2(*5H*)-furanones **3** and **6**. The main goal of this work is to assess the possibility of an extension of the rule to cover these 5-5-5 fused adducts also. Considering the increased rigidity of the structures analyzed, a smaller conformational effect should be expected in comparison to the earlier studied 6-5-5 fused systems derived from the six-membered lactones. On the other hand, the increased strain in 5-5-5 fused systems may affect the lactone ring conformation and cause a non-planarity of the chromophore. For these reasons, a detailed analysis of X-ray geometries of several cycloadducts was conducted. Furthermore, the influence of substituents on the shape of CD spectra was investigated. In the latter case, the effect of the substituent at the lactone ring and the presence of additional groups on the pyrrolidine ring were considered.

As we demonstrated recently,[14] the 1,3-DC reactions involving γ-lactones **3** and **6** display a lower diastereoselectivity in comparison to related reactions of their δ-analogues. In addition, we reported that in addition to the *exo* adducts, the *endo* adducts were also formed (for *exo*/*endo* definition see Scheme 1). In the latter case, the *endo* approach is strongly disfavoured because of the steric repulsion in the transition state.[15] The formation of *endo* adducts by furanones **3** and **6** enables us to examine their chiraloptical properties for the first time.

In addition, we intend to support the experimental studies with the quantum-mechanic simulations of CD properties of the analyzed cycloadducts. For this purpose, we decided to use DFT functional methods,[17] which are the most suitable for the analysis of electronic properties of organic compounds. These studies were preceded by a conformational analysis conducted applying molecular modelling methods. Furthermore, we decided to study the influence of additional chromophores (e.g., phenyl) present in the molecule on the electronic transitions of the lactone chromophoric system.

2. Results and discussion

2.1. Chiraloptical properties of *exo* adducts derived from 2(*5H*)-furanone 6

The CD data of *exo* adducts **8–21** (Chart 2) are collected in Table 1 (for *exo* definition see Scheme 1). The UV spectra of most adducts, except **8**, **14** and **17**, do not exhibit any characteristic absorption within the measurement range. As can be seen from Table 1, the CD spectra of **8–21** exhibit two CD bands between 211–220 nm and 189–199 nm. Based on the long-wavelength CD band sign, the compounds investigated can be divided into two groups. In the first group, represented by adducts **8–11**, **13–15** and **21**, the sign of this CE is negative, whereas in the second group (**16–20**) the sign of the CE is positive. These results correspond nicely to the trend observed previously for analogous adducts containing the six-membered lactone ring.[13] According to the respective NMR and X-ray[18] data for adducts **9**, **10**, **15**, **16** and **17**, the absolute configuration of compounds in the first group is (4*aR*), while the configuration of compounds in the second group is (4*aS*). A detailed investigation of the X-ray geometries of these cycloadducts revealed the planarity of lactone chromophoric system with the average value of dihedral angle O=C_4–O_3–C_2 close to ±177°. On this basis, we concluded that the ring-chirality rule is applicable to this class of 5-5-5 fused cycloadducts.

Further studies revealed that the rule is also applicable to adducts derived from the 5-substituted lactone **3**. Comparison of CD data of adducts **8** and **12** (Table 1, entry 1 and entry 14, Fig. 1)

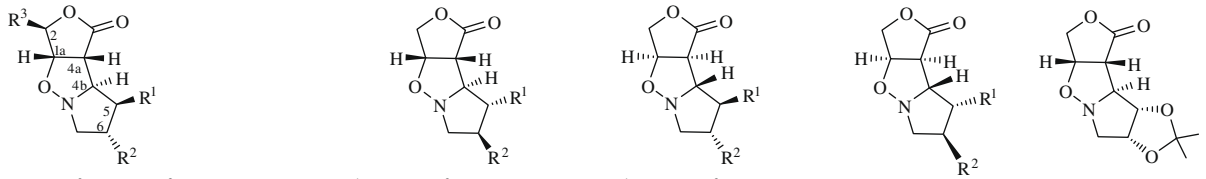

8 R^1: H R^2: H R^3: H
9 R^1: *t*-BuO R^2: H R^3: H
10 R^1: H R^2: *t*-BuO R^3: H
11 R^1: *t*-BuO R^2: *t*-BuO R^3: H
12 R^1: H R^2: H R^3: CH_2OH

13 R^1: *t*-BuO R^2: H
14 R^1: H R^2: *t*-BuO
15 R^1: *t*-BuO R^2: *t*-BuO

16 R^1: *t*-BuO R^2: H
17 R^1: H R^2: *t*-BuO
18 R^1: *t*-BuO R^2: *t*-BuO

19 R^1: H R^2: *t*-BuO
20 R^1: *t*-BuO R^2: *t*-BuO

21

Chart 2.

Table 1
UV and CD data of compounds **8**–**21** derived from lactone **6** recorded in acetonitrile

Entry	Compd	C_{4a}	CD $\Delta\varepsilon$ (λ)		
1	**8**[a,b]	(*R*)			−1.0 (217)
2	**12**	(*R*)			−1.0 (217)
3	**9**	(*R*)	+0.3 (189)		−1.8 (211)
4	**13**	(*R*)	+0.1 (190)		−1.5 (217)
5	**14**[c]	(*R*)	−1.9 (193)		−2.3 (219)
6	**10**	(*R*)	−2.1 (199)		−2.3 (212)
7	**11**	(*R*)	+0.9 (191)	−1.8 (204)	−2.5 (217)
8	**15**	(*R*)	−4.8 (191)		−2.7 (220)
9	**21**	(*R*)	(185)[e]	−2.3 (202)	−2.2 (211)
10	**16**	(*S*)	−0.1 (192)		+2.0 (216)
11	**17**[d]	(*S*)	+2.3 (193)		+2.5 (220)
12	**19**	(*S*)	+2.1 (198)		+2.2 (212)
13	**18**	(*S*)	+4.8 (191)		+2.8 (216)
14	**20**	(*S*)	−1.2 (191)	+2.0 (204)	+2.4 (216)

CD values are given as ε (λ/nm) and $\Delta\varepsilon$ (λ/nm), respectively.
[a] (*1aS,4aR,4bR*)-enantiomer.
[b] UV ε (λ) = 960 (195).
[c] UV ε (λ) = 1290 (193).
[d] UV ε (λ)= 560 (200).
[e] Negative inflexion point.

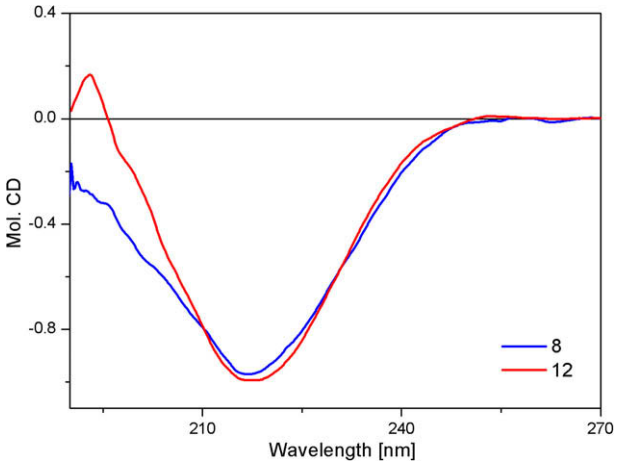

Figure 1. The CD spectra of compounds **8** and **12** recorded in acetonitrile.

showed that the introduction of a hydroxymethyl group on the lactone moiety does not affect the shape of the CD curve. This observation indicates a lack of the electronic influence and the steric hindrance of this substituent on the lactone chromophoric system. This is a general trend observed for all adducts derived from lactone **3**. As can be seen from the data collected in Table 1 and Figure 2, the substituents on the pyrrolidine ring have only a minor influence on the shape of CD curve and changes are observed in the range below 205 nm only.

To exclude the possible solute-solvent interactions, which could have an effect on the CD spectra, the CD measurement for adducts **10**, **15**, **16** and **17** were also performed in solid state (nujol mull). In all cases, the solid-state data were in an excellent agreement with the respective data recorded in solution (Fig. 3). Accordingly, it can be concluded that the same molecular species are present both in solution and in the solid state and only one conformer is present, or predominates strongly, in solution. Such a good agreement of CD data obtained by different measurement techniques indicates that the determination of absolute configuration of adducts **8–21**, as well as of those derived from lactone **3**, can be performed on the basis of the chiraloptical data measured in solution.

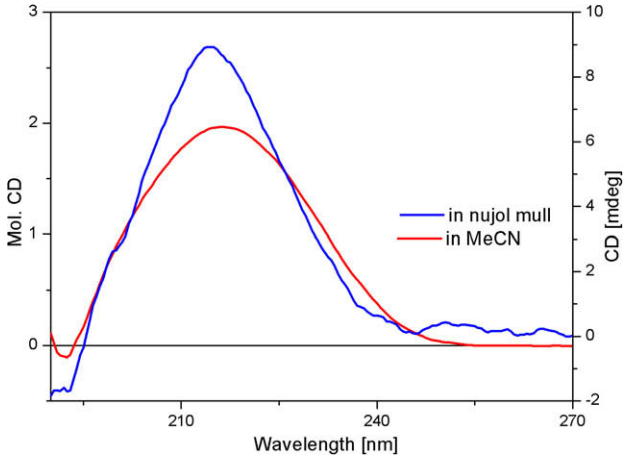

Figure 3. The CD spectra of cycloadduct **16** recorded in acetonitrile solution and nujol mull.

2.2. Chiraloptical properties of *endo* adducts derived from 2(*5H*)-furanone 6

The CD and UV data for *endo* adducts **22–29** (Chart 3, for *endo* definition see Scheme 1) are collected in Table 2. Generally, the CD spectra exhibit two CD bands at around 204 nm and 190 nm (Fig. 4). An exception with respect to the position of the long-wavelength CD band is found for compound **29**. In this single case, the band is shifted to 235 nm (Fig. 4).

The inspection of data collected in Table 2 demonstrated that the sign of long-wavelength band depends on the configuration at the C-4a carbon atom. Analogously to the *exo* adducts, the *endo* adducts can be divided into two groups. In the first group, compounds **22–26** and **29**, the sign of this band is negative whereas

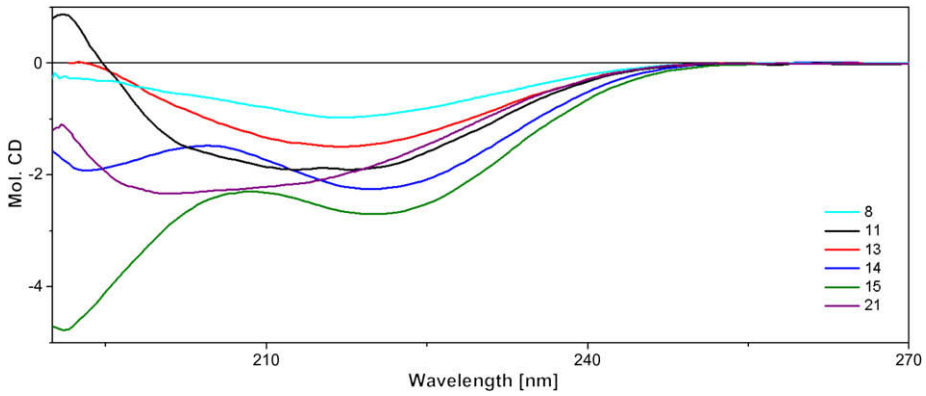

Figure 2. The CD spectra of adducts **8**, **11**, **13–15** and **21** taken in acetonitrile.

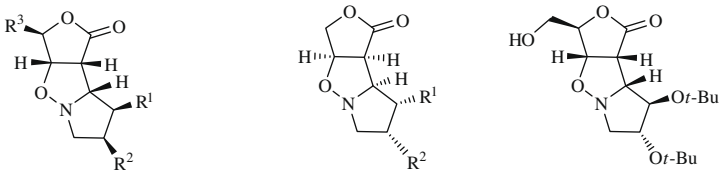

22 R^1: *t*-BuO R^2: H R^3: H
23 R^1: H R^2: *t*-BuO R^3: H
24 R^1: H R^2: H R^3: CH_2OH
25 R^1: *t*-BuO R^2: H R^3: CH_2OH
26 R^1: H R^2: *t*-BuO R^3: CH_2OH
30 R^1,R^2,R^3: H

27 R^1: *t*-BuO R^2: H
28 R^1: H R^2: *t*-BuO

29

Chart 3.

Table 2
UV and CD data of *endo* adducts **22**–**29** derived from lactones **3** and **6** recorded in acetonitrile

Entry	Compd	C_{4a}	UV ε (λ)		CD $\Delta\varepsilon$ (λ)
1	**22**	(*R*)	2750 (195)		−3.5 (205)
2	**23**	(*R*)	2100 (195)	−4.0 (187)	−4.3 (203)[sh]
3	**24**	(*R*)	[a]		−1.9 (204)
4	**25**	(*R*)	[a]	−4.9 (192)	−3.5 (204)
5	**26**	(*R*)	3030 (196)	(190)[b]	−3.5 (205)
6	**29**	(*R*)	800 (193)	+0.4 (197)	−0.7 (235)
7	**27**	(*S*)	[a]		+3.1 (204)
8	**28**	(*S*)	[a]		+4.3 (203)

UV and CD values are given as ε (λ/nm) and $\Delta\varepsilon$ (λ/nm), respectively.
sh: Shoulder.
[a] No characteristic absorption in measurement range.
[b] Positive inflexion point.

Table 3
Basis-set saturation effect on calculated n→π* transition of a lactone chromophore for **8**

Basis set	Transition n→π*			
	λ (nm)	*f*	R_{vel}	%[a,b]
6-31G(d)	225	0.0006	−3.3	66(6)
6-31+G(d,p)	225	0.0005	−3.1	65(6)
6-31++G(d,p)	225	0.0006	−7.8	67(6)
6-31++G(2d,p)	225	0.0006	−8.3	67(6)
6-311G(d,p)	225	0.0007	−6.1	68(5)
6-311+G(d,p)	226	0.0005	−6.7	68(6)
6-311++G(d,p)	226	0.0005	−7.1	67(5)
6-311G(2d,p)	225	0.0007	−7.3	68(5)
6-311+G(2d,p)	226	0.0005	−6.3	68(6)
6-311++G(2d,p)	226	0.0007	−10.5	66(6)

[a] A content of the n→π* transition of lactone chromophore in simulated transition.
[b] In parentheses content of the π→π* transition of the lactone chromophore in simulated transition.

in the second group, adducts **27** and **28**, the sign is positive. Considering the NMR and X-ray data for adducts **22** and **25**,[19] it can be assumed that the negative sign of the ca. 204 nm CD band corresponds to the (4*aR*)-absolute configuration. Therefore, for the second group displaying a positive sign of the same band, the (4*aS*)-absolute configuration should be expected (see Table 2).

In comparison to the CD spectra of *exo* adducts discussed earlier, the long-wavelength CD band is blue-shifted by about 10 nm. It seemed possible that in the *endo* adducts the close proximity of lactone and pyrrolidine rings would cause a slight deformation of the 5-5-5 fused system to minimize the repulsion between both rings. Therefore, a distortion of the lactone rings leading to some non-planarity of the chromophore could be expected. Detailed analysis of the X-ray geometries of **22** and **25**, however, showed that for both compounds the dihedral angle O=C_4–O_3–C_2 equal to 177° was found. On this basis, it can be concluded that the ring-chirality rule should be applicable to the *endo* adducts also.

The X-ray data for compound **25** provide additional evidence supporting the configurational assignment. The ORTEP representation shown in Figure 5 clearly demonstrates the (4*aR*)-absolute configuration in accordance to our prediction made on the basis on the CD data. Due to the excellent agreement between CD curves for **25** recorded in solution and in nujol mull (Fig. 6) we can assume that the same molecular species are present in both states. Therefore, adduct **25** can be considered as a model compound in the determination of the absolute configuration for remaining compounds reported in Table 2.

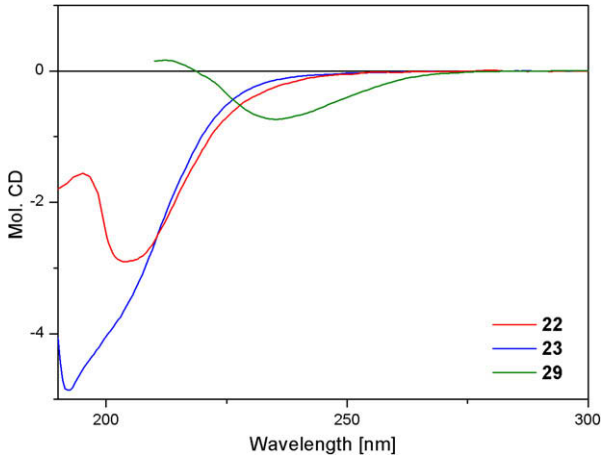

Figure 4. The CD spectra of compounds **22**, **23** and **29** recorded in acetonitrile.

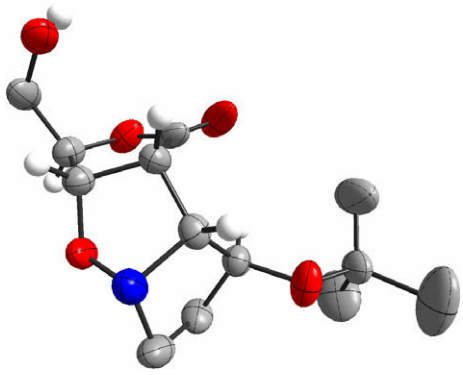

Figure 5. ORTEP representation of compound **25** (for clarity some hydrogen atoms are omitted).

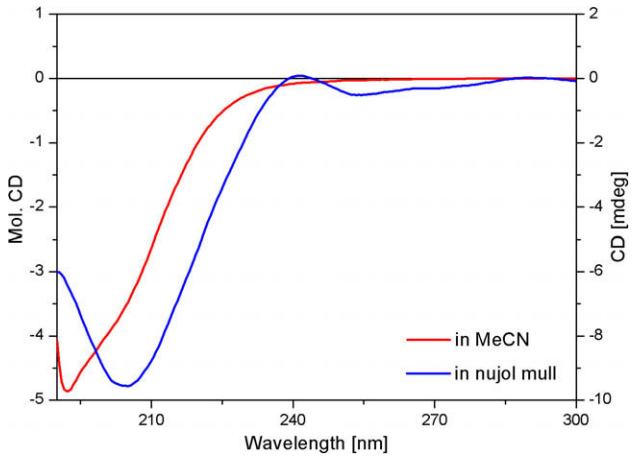

Figure 6. The CD data of adduct **25** recorded in acetonitrile solution and in solid state (nujol mull).

The observed difference in position of the n→π* bands between *exo* adducts and *endo* adducts may be caused by the specific arrangement of the lactone and the pyrrolidine rings. Conformational analysis of model adduct **30**, without any substituents attached to the 5-5-5 ring fused system,[15b] as well as of adduct **22**, revealed that the isoxazolidine ring adopts an envelope conformation with the co-planar arrangement of C-1a, C-4a, C-4b and N-8 atoms. The O-1 atom is localized between both five-membered rings (Fig. 7). Such an arrangement minimizes the steric repulsion between the lactone and pyrrolidine rings. A detailed analysis of the lowest-energy conformers of **30** and **22** suggests a possible interaction between the carbonyl group and hydrogen atom at C-5, which may affect the electronic transitions of this chromophore group (Fig. 7). In addition, for compound **22**, there is also indication of some steric repulsion involving protons of the *tert*-butyl group (Fig. 7).

The red-shift (approx. 30 nm) of the n→π* CE observed for adduct **29** can be caused by the perpendicular arrangement of the pyrrolidine and lactone rings, according to the molecular modelling calculations. The electronic repulsion of 6-O*t*-Bu and the carbonyl group causes a distortion of the lactone ring as can be seen in Figure 8. Thus, the dihedral angle, usually falling within 174–177° range, here is found to be 167° only. For this reason, the ring-chirality rule is not applicable to this molecule.

2.3. Theoretical investigation of the Legrand–Bucourt empirical rule

The effectiveness of the Legrand–Bucourt empirical rule in the determination of the chiraloptical properties of various lactones has been demonstrated repeatedly.[13a,b,20] As mentioned before,

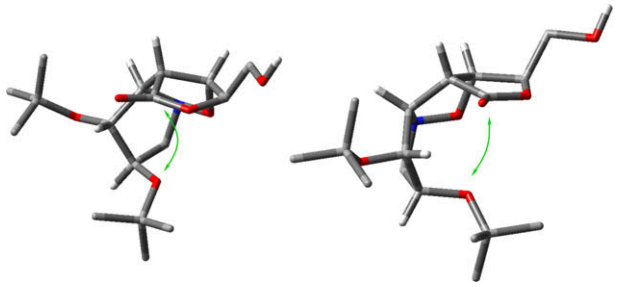

Figure 8. The lowest-energy conformer of adduct **29** (two projections are shown).

the rule assumes the planarity of lactone chromophore and the lack of electronic influence of other components of the molecule on the lactone chromophore. The difficulties arise when an additional strong chromophore is present in the molecule. These questions prompted us to undertake an investigation of the origin of the ring-chirality rule applying quantum-mechanic calculation. Several of the earlier discussed cycloadducts were chosen as a calculation model. The presence of heteroatoms makes these molecules particularly attractive for such a purpose. Moreover, a comparison of the influence of different substituents on the net CD is possible by simple modification of the hydroxy group protection.

Taking into consideration the fact that the electronic properties of organic compounds are determined by their electronic structure, a density functional theory has been chosen as the most adequate calculation method for this purpose. Initially, the simplest adduct **8** was chosen as a model for theoretical studies.

The experimental CD spectrum of adduct **8** in acetonitrile is shown in Fig. 9. The observed broadening of CD band may indicate

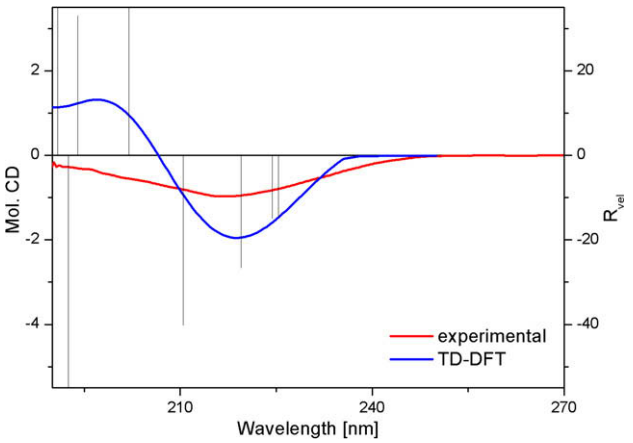

Figure 9. Experimental and theoretical CD spectra of compound **8**.

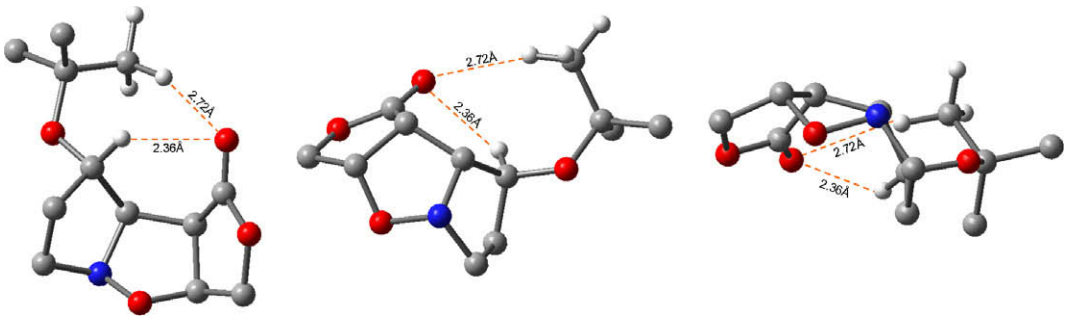

Figure 7. The lowest-energy conformer of adduct **22** (three projections are shown). For clarity, some hydrogen atoms are omitted.

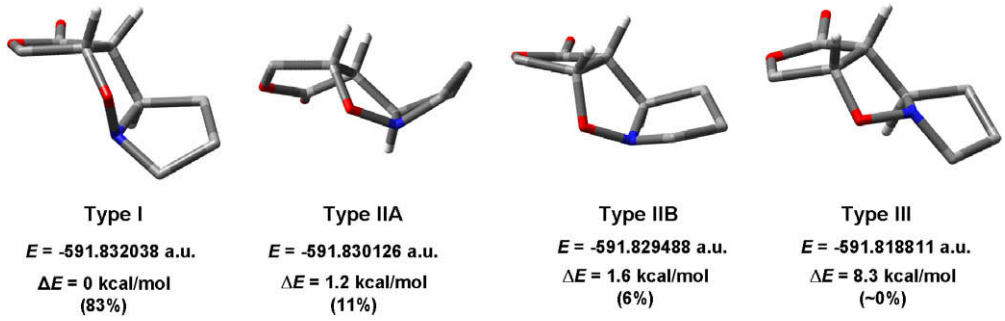

Figure 10. Conformers of compound **8** (for clarity some hydrogen atoms are omitted). Total energies, relative energies and Boltzmann statistic (in parentheses) are given.

the presence of several (at least two) electronic transitions differing only slightly in energy. For certain lactone chromophores, the $n\rightarrow\pi^*$ transition overlaps the respective $\pi\rightarrow\pi^*$ transition because of their similar energy.[21] Therefore, the poorly resolved CD bands are observed in the spectrum. To provide evidence for this statement the MO theoretical calculations were performed.

Before simulation of the CD spectrum of **8,** the conformational aspects were evaluated by applying the combination of molecular mechanics and DFT calculations. The conformational search was carried out using MM+ force field.[22] The low conformational lability of five-membered fused ring system makes it rather rigid, and only a few conformers within the range of 10 kcal/mol were found. The resulting conformers were further re-optimized by the DFT calculations at B3LYP/6-31+G(d) level of theory (in vacuo), resulting in the structures shown in Figure 10 as the lowest-energy minima.[15b] These conformers can be divided into three types with respect to the isoxazolidine ring. The co-planar arrangement of C-1a, C-4a, C-4b and O-1 atoms in type **I** conformer ensures the planarity of lactone moiety (Fig. 10). On the other hand, for type **II** conformers, the oxygen atom O-1 is out-of-plane formed by C-1a, C-4a, C-4b and N-8 and therefore the lactone ring is not planar.[15b] Type **II** conformers differ mostly in the conformation of the pyrrolidine ring. Structures **IIA** and **IIB** have higher energies (Fig. 10) with respect to the conformer **I** and are negligible in the Boltzmann population at room temperature. The low conformational lability of the 5-5-5 fused system also prevents free inver-

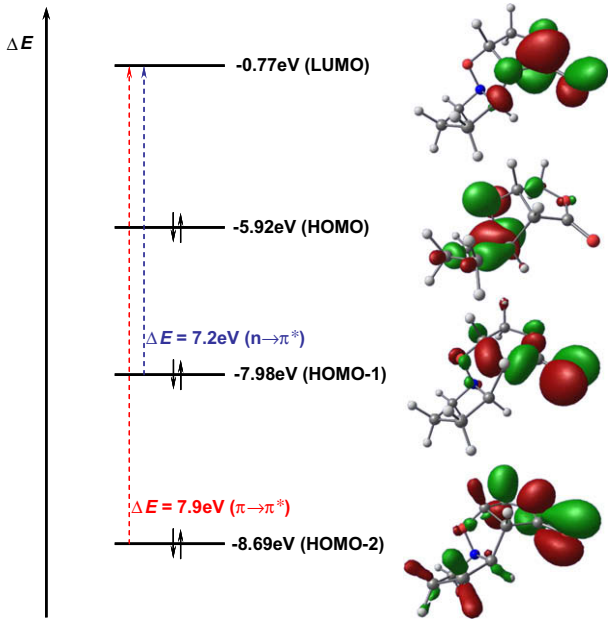

Figure 11. Molecular orbitals involved in transitions of compound **8**.

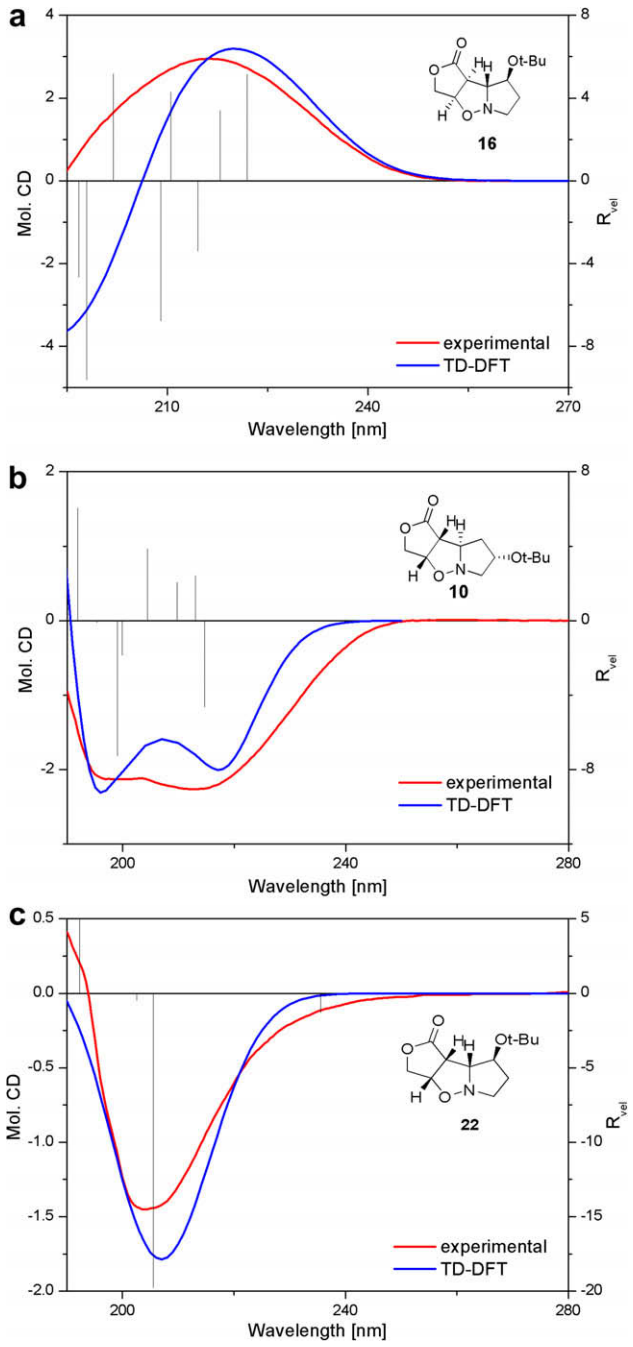

Figure 12. Experimental and theoretical CD spectra of (a) adduct **16**; b) adduct **10** and c) adduct **22**. In all cases a rotatory strength R_{vel} was included.

Table 4
UV and CD data of compounds **31**–**34** derived from nitrone **7** recorded in acetonitrile[a]

Entry	Compound	C_{4a}	UV ε (λ)	CD Δε (λ)			
1	**31**	(*S*)	9900 (207)	−3.9 (182)	+8.3 (193)	+2.7 (212)^{sh}	−0.5 (228)
2	**32**	(*R*)	11,000 (205)	+1.4 (191)	−0.6 (198)	+0.7 (213)	+0.6 (223)
3	**33**	(*S*)	9010 (205)	−1.1 (184)	+6.8 (192)	+1.1 (213)^{sh}	−0.8 (225)
4	**34**	(*R*)	1800 (206)	+0.8 (190)	+0.1 (198)	+0.2 (212)	+0.2 (223)^{sh}

UV and CD values are given as ε (λ/nm) and Δε (λ/nm), respectively.
sh: shoulder.
[a] An additional low-intensity band corresponding to ^1L_b transition of the phenyl group was observed at around 257 nm.

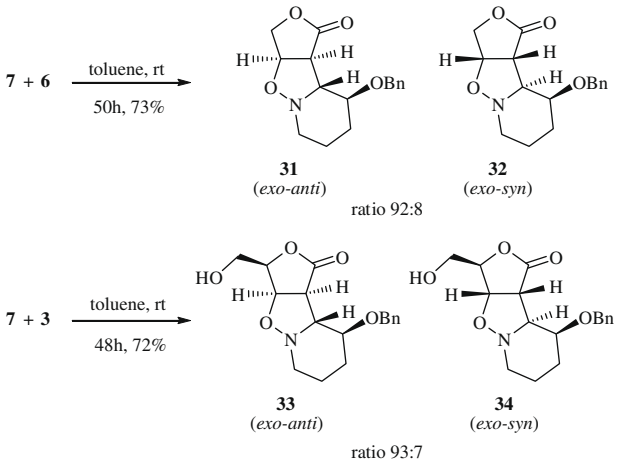

Scheme 2.

sion at the nitrogen atom. Thus, the *cis* arrangement of the nitrogen lone pair and the H-4b atom is observed which was corroborated by both X-ray analysis[18] and the conformational search for numerous cycloadducts. The conformer with the *trans* arrangement of the nitrogen lone pair and the H-4b proton (Fig. 10, **III**) is substantially higher in energy (ca. 8.3 kcal/mol) with respect to all other conformers[15b] and therefore has no significance for the chiraloptical properties. Such a result is in accordance with previous NMR studies carried out by Font and de March.[23]

For the lowest-energy conformer of **8** (conformer **I**), the absorption and CD spectra have been calculated applying the time-dependent DFT (TD-DFT)[24] method using B3LYP functional and different basis sets (Table 3). For the treatment of the solvent effect, the polarized continuum model (PCM)[25] method was used with acetonitrile as the solvent. The calculations were carried out using the GAUSSIAN 03 suite of quantum chemical programs.[26]

The analysis of the basis-set saturation effect gave similar results (Table 3) showing only small basis-set dependence on the calculated transitions. According to the results obtained, for further CD curve simulations a B3LYP/6-311+G(d,p) level of theory has been chosen. The simulated and experimental CD spectra of **8** (conformer **I**) are shown in Figure 9. Both experimental and theoretical curves are in a good agreement. Detailed analysis of the lowest-energy transitions in the spectral range from 209 to 225 nm confirms their complex character. However, the most important electronic transition (HOMO-1→LUMO) was found to have mostly the n→π* character. For example, its content at 225 nm is 68% and at 219 nm it is 22%. As an additional component, the π→π* transition was found, however, its contribution is lesser. Figure 11 presents molecular orbitals involved in the transitions of compound **8**. As shown in Figure 11, the molecular orbitals participating in the transition of the chromophore group have a complex character with a large contribution of the carbonyl group orbitals. The energy for the n→π* and π→π* transitions equals 7.2 and 7.9 eV, respectively. The energy difference is only 0.7 eV thus confirming the previous prediction.

This result suggests that Legrand and Bucourt's assumption about the lack of a significant influence of other atoms on the chiraloptical properties of the lactone cannot be true since the observed transitions constitute a mixture of several transitions stemming from various molecular components. Of course, it should be taken into account that their relative contributions depend on their distance to the lactone chromophoric system.

In continuation of the theoretical studies, adducts bearing additional substituents were investigated. As it was pointed out earlier, the presence of an additional hydroxymethyl substituent near the lactone moiety does not affect the chiraloptical properties of the studied adducts. For this reason, only compounds with an RO-substituent at the pyrrolidine ring were taken into consideration and compounds **10**, **16** and **22** were chosen as models. For all of them, the DFT optimization was carried out using X-ray geometries as an input. In all cases, the computationally optimized geometry and the structure obtained by the X-ray were similar.

Based on the conformational search for adduct **16**, five minima were found, but only the global minimum was considered for further studies (the difference in energy of other structures exceeds 2 kcal/mol, so they do not have a significant thermal population at room temperature).[15] Figure 12a shows simulated and experimental spectra of compound **16**, with both curves being in a good agreement.

The transposition of the substituent from C-5 in **16** to C-6 in **10** changed the shape of the CD curve (Fig. 12b). The adduct **10** shows two negative poorly resolved bands, in contrast to the CD curve of **16** showing only one broadened band. For the lowest-energy conformer of **10**, the simulated curve is in very good agreement with the experimental spectrum, as can be seen in Figure 12b.

As was discussed earlier, the *endo* adducts feature a characteristic increase in energy of the n→π* transition that is manifested in the presence of appropriate CE in spectral range of 203–205 nm. As can be seen in Table 2 and Figure 12c, the CD curve of adduct **22** contains one broadened negative band at 205 nm. The simulated curve shown in Figure 12c is in excellent agreement with the experimental one.

The agreement above between simulated and experimental CD spectra confirms the accuracy of Legrand and Bucourt rule by both experiment and theory.

2.4. Chiraloptical properties of adducts derived from 2(*5H*)-furanones and six-membered nitrone 7

Next, the experimental and theoretical studies of systems containing an additional strong chromophore were carried out. For this purpose, four adducts shown in Scheme 2 were selected.[†]

[†] The reaction of chiral nitrone **7** with achiral lactone **6** afforded a mixture of two exo products **31** and **32** in a ratio of 92:8 (HPLC) and 73% yield (Scheme 2). The absolute configuration of products was assigned analyzing the NMR spectra. Additionally, the configurational assignment of **31** is supported by the X-ray analysis (Fig. 13). The replacement of achiral lactone **6** by its chiral analogue **3** did not significantly change the outcome of reaction and again two products **33** and **34** were obtained (ratio 93:7, yield 72%; Scheme 2). As in the previous experiment, the major product was identified as an *exo-anti* adduct and the minor one as an *exo-syn* isomer.

In Table 4, a summary of the relevant UV and CD data of adducts **31–34** is given. Apparently, the presence of a hydroxymethyl group at the lactone moiety had no significant influence on the dichroic spectra of the investigated molecules.

According to data recorded in Table 4, the CD curves of adducts **31–34** are characterized by four CEs at around 186, 195, 213 and 225 nm. Such a complex character of the CD curves may indicate that the MOs of the lactone chromophore mix strongly with the MOs localized at the benzyloxy chromophore. This observation is in an agreement with our theoretical calculation of molecular orbitals for **31** (vide infra).

As indicated in previous paragraphs, the base transition of the lactone unit ($n\rightarrow\pi^*$) is observed at around 215 nm. On this basis, it was assumed that for adduct **31** the CE at 212 nm corresponds to this transition. Moreover, the positive sign of this band, corresponding to the (4*aS*)-absolute configuration corroborated our previous conclusion, based on the X-ray geometry (Fig. 13), that compound **31** obeys the Bucourt–Legrand rule. The CD band at around 228 nm originates most probably from the $\pi\rightarrow\pi^*$ transition of benzyloxy group.

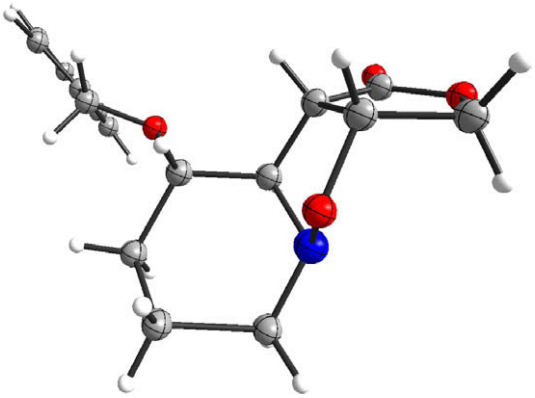

Figure 13. The ORTEP representation of compound **31**.

The conformational analysis of compound **31** revealed three low-energy conformers (Fig. 14). Type **I** conformer has a planar lactone ring and the chair conformation of piperidine ring with an equatorial BnO substituent. The planarity of lactone chromophore was also observed for the type **II** conformer. The axial arrangement of the BnO group increased, however, its energy with respect to the conformer **I** by 2.5 kcal/mol. Therefore, conformer **II** was omitted from further discussion owing to its presumed negligible contribution to the Boltzmann population at room temperature.

The type **III** conformer, with the *trans* arrangement of H-4b and nitrogen's lone pair, is only slightly more energetic when compared to the conformer **I** (ΔE 0.9 kcal/mol). According to the theoretical calculations, approximately 20% content of **III** in the conformational equilibrium should be expected. However, this

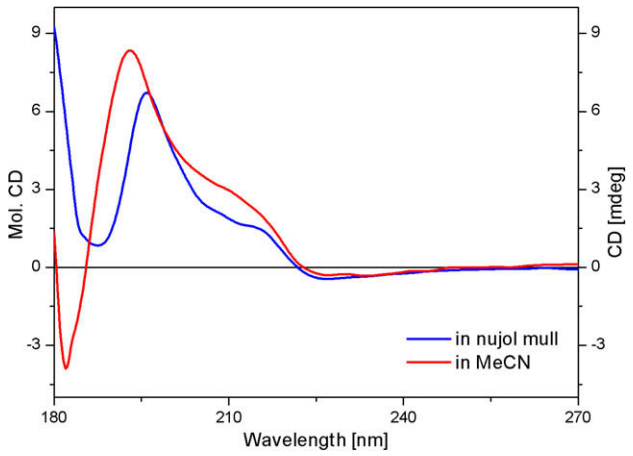

Figure 15. The CD data of **31** recorded in solution and in solid state.

conclusion contradicts the experimental data available for **31**. The similarity of the CD curves of **31** recorded in acetonitrile solution and nujol mull (Fig. 15) allowed us to conclude that in both states, the same molecular system is present. Moreover, the temperature-dependent CD measurements suggest strongly the predominance of one conformer in solution.

The re-calculation of energy for type **I** and type **III** conformers of **31** with the higher basis set increased the relative energy difference from 0.9 to 1.0 kcal/mol which indicates the decrease of conformer **III** content from 20% to 15% only.

Figure 16a and b show the simulated CD curves for both conformers **31-I** and **31-III**, respectively. Due to the planarity of lactone chromophore in **31-III**, this conformer was considered in the simulation of weight-average CD curve with respect to the Boltzmann distribution of conformers (85:15). Both experimental and average theoretical curves are in a satisfactory agreement (Fig. 16c).

A detailed analysis of the calculated transitions in the spectral range from 210 to 240 nm confirms their complex character and the strong interference of the phenyl chromophore with the lactone moiety. The molecular orbitals involved in the most important transitions of both chromophores for compound **31** are shown in Figure 17. As in the previous examples (Fig. 11), the lactone orbitals (π, n and π^*) are an admixture with a large contribution of orbitals from other components of the molecule. The calculation proves that the transition at around 230 nm corresponds to the $\pi\rightarrow\pi^*$ electronic transition of the phenyl group. This transition is an admixture of energetically close transitions (from HOMO, HOMO-1, HOMO-2 to LUMO, LUMO+1, LUMO+2). The lactone $n\rightarrow\pi^*$ transition can be found at around 213 nm which confirms the previous assumption based on the correlation of experimental data of **31** with 5-5-5 fused series of compounds **8–21**. However, these molecular excitations are not localized but couple with both phenyl $\pi\rightarrow\pi^*$ and lactone $\pi\rightarrow\pi^*$ transitions.

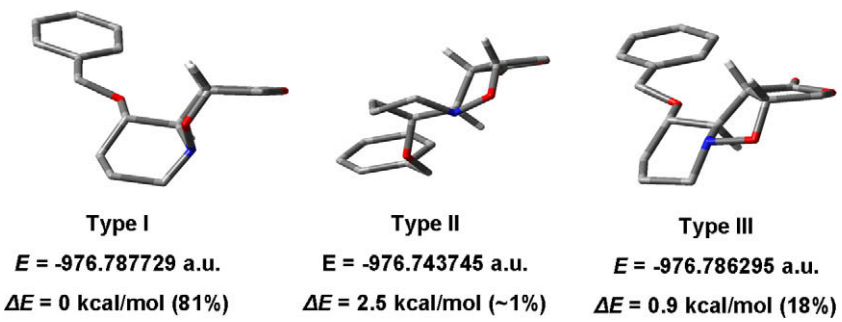

Figure 14. Conformers of compound **31** (for clarity some hydrogen atoms are omitted). Total energies, relative energies and Boltzmann statistic (in parentheses) are given.

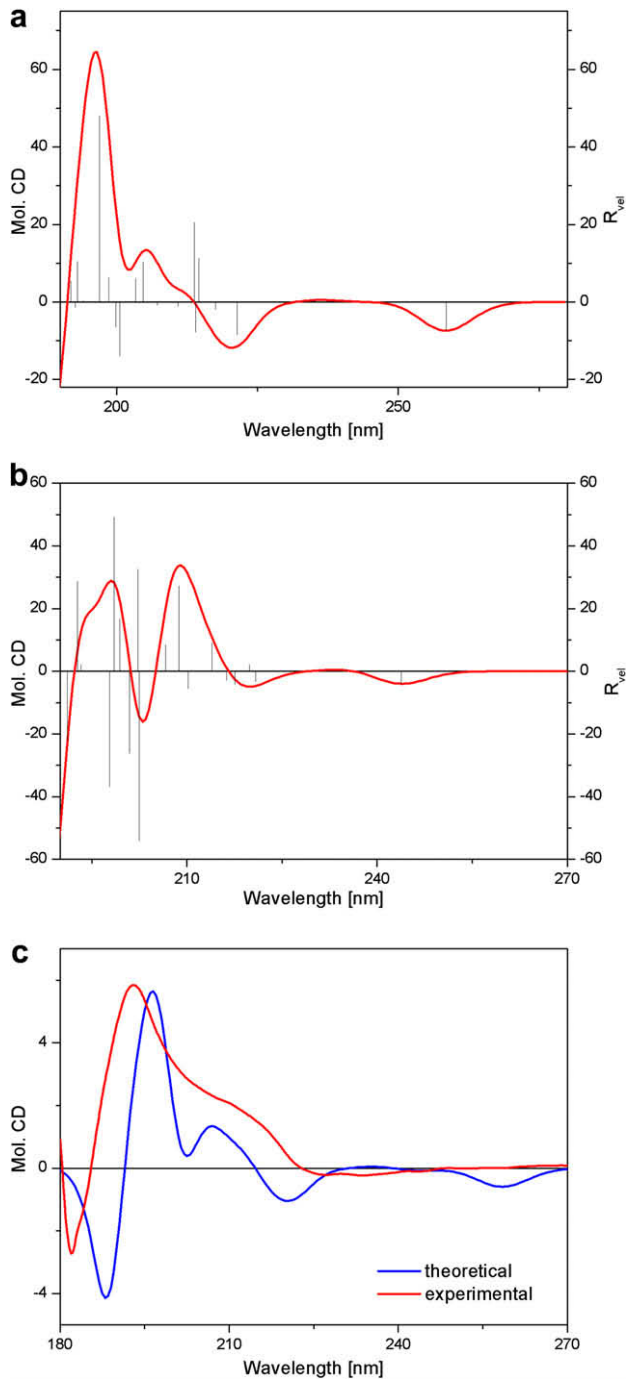

Figure 16. (a) Simulated CD curve for conformer **I**; (b) simulated CD curve for conformer **III** and (c) experimental and simulated CD curves for adduct **31**.

The situation is more complex for the *exo-syn* adduct **32** (Table 4). As shown for earlier examples, for adduct with (4*aR*)-configuration, a negative band in the spectroscopic range 210–220 nm should be present. Unexpectedly, the CD curve of compound **32** recorded in acetonitrile has a positive CE in this range. This may suggest that the ring-chirality rule is not applicable to compounds **32** and **34** (Fig. 18). However, the low intensity of the CD band at 213 nm may indicate that in the solution, a mixture of at least two conformers is present. Indeed, when the CD measurements were done in nujol mull or KCl pellet, the change of the sign of the bands above 205 nm was observed (Fig. 18). The negative sign of the band at around 208 nm nicely corresponds to the prediction made for (4*aR*)-configuration. The discrepancy observed for the CD data recorded in solution and in solid state indicates that a different molecular species exists in both states. Such an extraordinary behaviour of adduct **32** may be caused by the interaction of the benzyloxy group and the lactone ring which is advantageously situated for the presumed orbital overlapping.

The above unexpected observations were confirmed by conformational analysis. All three conformers which were found for adduct **32** are depicted in Figure 19. Structures **I** and **II** are equal in energy and represent the global minima, whereas the invertomer **III** is higher in energy by about 3.3 kcal/mol, and can be omitted because of a presumed lack of significant contribution to the Boltzmann distribution of conformers. An increased energy for **III** is a function of the electronic repulsion between the lone pair of nitrogen and both lone pairs of oxygen atom within the BnO group. To minimize this interaction, the piperidine ring adopts a twist-boat conformation.

As mentioned before, both predicted conformers **I** and **II** are energetically equal. In case of conformer **I**, the more favourable conformation of the isoxazolidine ring results in the piperidine ring adopting the $_4C^1$ chair conformation with an unfavourable axial arrangement of the BnO substituent. In the case of conformer **II** with an equatorial BnO substituent and $^4C_1$ conformation of the piperidine ring the isoxazolidine ring adopts a less preferred conformation with the O-1 oxygen atom out of the envelope plane. In both cases (**I** and **II**), the lactone chromophore system is planar. Additionally, the proximity of the oxygen atom of the benzyloxy group and the relatively acidic H-4a proton may indicate a possible internal hydrogen-bonding type interaction which may stabilize the adduct's conformation. Very recently, we postulated an analogous interaction for the structurally related adduct **9**, which was corroborated by the NMR and DFT studies.[15b] However, a detailed comparison of conformers of **32** with those obtained for **9** suggests that this extra stabilization is weaker in adduct **32** because of the less effective overlapping of interacting orbitals.

Both the simulated and experimental CD spectra for conformers **I** and **II** of adduct **32** are presented in Figure 20. Their comparison revealed that the simulated CD curve of **I** corresponds better to the solution data whereas the simulated CD curve of **II** has a shape that is similar to that of the curve recorded in the solid state. Based on this result, it can be concluded that conformer **I** predominates in solution whilst conformer **II**, with an equatorial BnO substituent, is present in the solid state. Unfortunately, we could not confirm this conclusion by X-ray analysis because compound **32** does not form suitable crystals.

Analogously to adduct **31**, the computational investigation of MOs of **32** confirmed the complex character of experimentally observed electronic transitions by showing the strong interference of the phenyl group localized MOs and base transitions of the lactone chromophore system.

To conclude, adducts **31** and **33** obey the Bucourt–Legrand rule whereas compounds **32** and **34** do not comply with the rule. This is most likely because of the specific stereochemical arrangement of the interacting chromophores, namely, the lactone unit and the benzyloxy group.

3. Conclusions

Herein, the relationship between the molecular structure and the chiroptical properties of 5-5-5 and 5-5-6 fused heterocyclic systems, derived from the five- and six-membered cyclic nitrones and 2(*5H*)-furanones, was investigated by electronic circular dichroism spectroscopy, time-dependent density functional theory, molecular modelling calculations and the X-ray diffraction analysis.

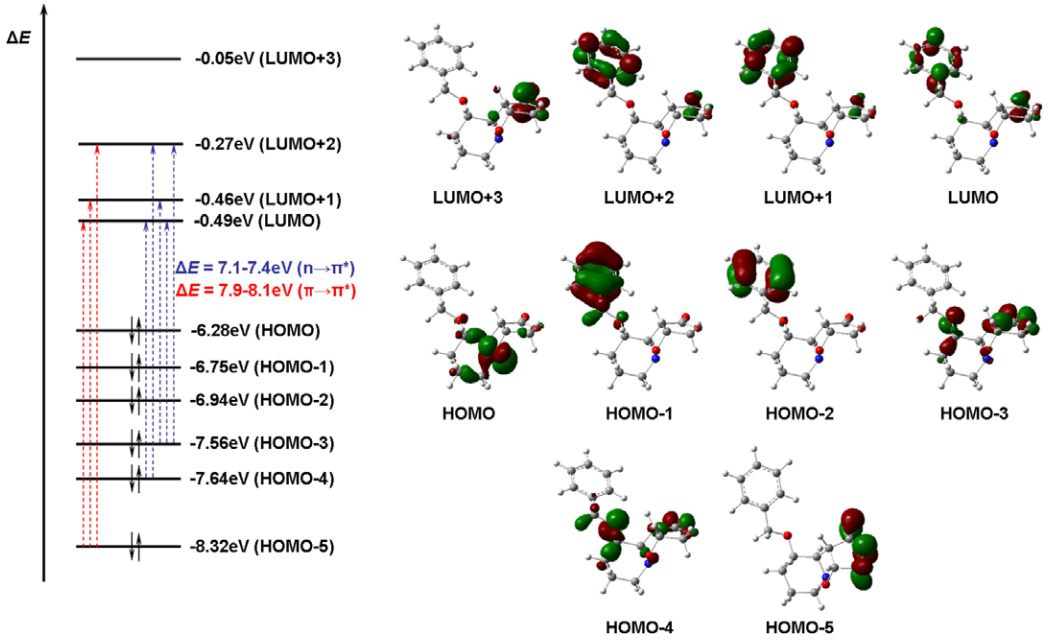

Figure 17. Molecular orbitals involved in transitions of compound **31**.

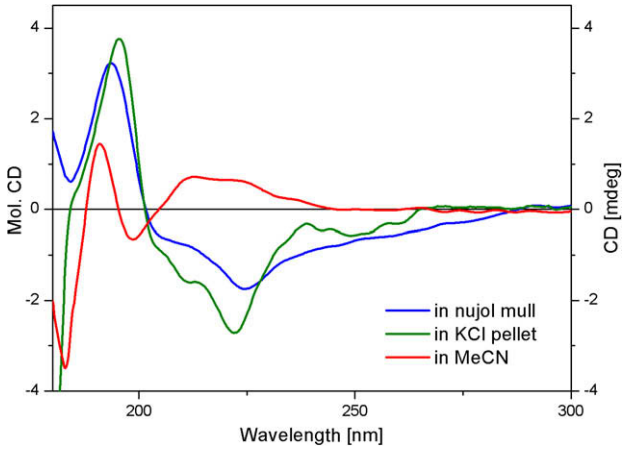

Figure 18. The CD data of **32** recorded in MeCN and in solid state (nujol mull and KCl pellet).

The comparison of experimental data for the *exo* adducts and *endo* adducts in 5-5-5 fused series of compound revealed significant difference in the position of the long-wavelength band which may serve as a useful indicator during the assignment of configuration. A characteristic blue-shift of the CD band for *endo* adducts was confirmed by theoretical calculation using DFT methods.

The computed O=C_4–O_3–C_2 dihedral angle provides the corroborating evidence for the planarity of the lactone chromophore. The band at around 213 nm (or 204 nm for *endo* adducts) has mainly the $n\rightarrow\pi^*$ transition character. Its positive or negative sign, contingent upon the (*4aS*)- or (*4aR*)-absolute configuration, respectively, is predicted by both the Bucourt–Legrand rule and the TD-DFT calculations, in most cases. Generally, the agreement between the simulated and the experimental ECD spectra was very satisfactory and demonstrates that the rule can be successfully applied to the assignment of the absolute configuration of the investigated 5-5-5 fused cycloadducts. However, the CD spectra of 5-5-6 fused adducts with an additional benzyloxy substituent are particularly sensitive to the changes of the molecular conformation. The different conformers of the same adduct can have a radically different CD spectrum. In some cases, a difference between solution and solid-state CD spectra was observed proving that the different molecular species (conformers) are present in both states. Moreover, the presence of an additional chromophore group complicates the CD spectra due to its interference with the lactone chromophore. Therefore, to successfully apply the Bucourt–Le-

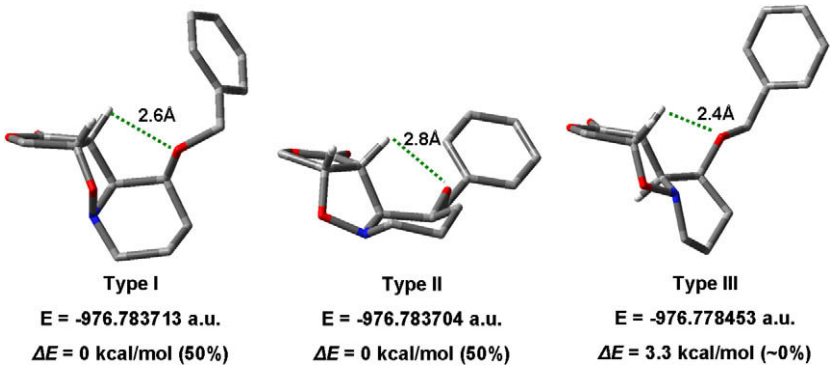

Figure 19. Conformers of adduct **32**. Total energies, relative energies and Boltzmann statistic (in parentheses) are given.

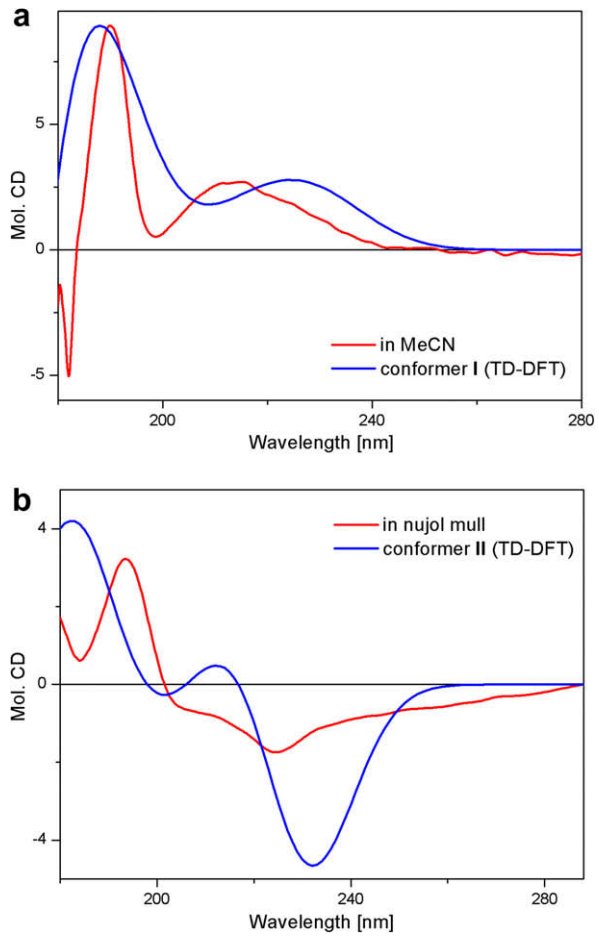

Figure 20. Experimental and simulated CD curves for adduct **32**; (a) CD data recorded in MeCN and simulated CD curve for conformer **I**; (b) CD data recorded in nujol and simulated CD curve for conformer **II.**

grand rule for the unequivocal configurational assignment, the TD-DFT calculations are strongly recommended to support the conclusions are strongly recommended.

4. Experimental

4.1. General methods

Melting points were determined using Köfler hot-stage apparatus with microscope and are uncorrected. Proton and carbon NMR spectra were recorded on a Bruker DRX 500 Avance Spectrometer at 500 MHz and 125 MHz, respectively, using deuterated solvents and TMS as an internal standard. Chemical shifts are reported as δ values in parts per million and coupling constants are in Hertz. Infrared spectra were recorded on an FT-IR-1600 Perkin–Elmer spectrophotometer. The optical rotations were measured with a JASCO J-2000 digital polarimeter. High resolution mass spectra were recorded on ESI-TOF Mariner spectrometer (Perspective Biosystem). The HPLC analysis was carried out on Hitachi chromatograph with L-2130 pump and L-2450 DAD detector equipped with a LiChrospher® Si60 analytical column.

Thin layer chromatography (TLC) was performed on aluminium sheets Silica Gel 60 F_{254} (20 × 20 × 0.2) from Merck. Column chromatography was carried out using Merck silica gel 230–400 mesh. The TLC spots were visualized in UV (254 nm) and by treatment with alcoholic solution of ninhydrine, aqueous solution of $KMnO_4$ or with ceric sulfate/phosphomolybdenic acid solution.

Nitrone **7** was prepared following the literature procedure.[27] Compounds **8–29** were prepared following our previously published procedures.[14]

Cycloadduct **13** was obtained following the reported procedure[23] starting from nitrone **6** and lactone **11**. The enantioenriched sample of **13** (0.5 mg, ee 90%) was obtained by HPLC using Chiralcel® OD-H (Daicel) column (eluent: hexane/*i*-propanol 60:40 v/v, flow 1 mL/min, UV detection at 195 nm). Retention times: 7.3 min for (*1aR,4aS,4bS*)-***ent*-13** and 8.2 min for (*1aS,4aR,4bR*)-**13**.

4.2. Cycloaddition of nitrone 7 to lactones 3 and 6. General method

To a solution of the lactone (0.36 mmol) in toluene (3 mL, anhydrous) a solution of nitrone **7** (0.47 mmol) in toluene (2 mL) was added and the mixture was stirred under argon. The progress of reaction was monitored by TLC. After complete consumption of the lactone, the reaction mixture was concentrated and the residue was chromatographed on a silica gel using hexane/ethyl acetate mixture (1:1 v/v, for lactone **6** or 1:2 v/v, for lactone **3**) as an eluent. The cycloadducts' ratio was assigned by the HPLC. The assignments of NMR peaks were performed by using COSY experiments.[‡]

4.2.1. (1*aR*,4*aS*,4*bS*,5*R*)-5-Benzyloxy-octahydrofuro[3,4-d]pyridin[1,2-*b*]isoxazol-4(3H)-one 31

Colourless crystals, mp 77–79 °C (benzene); $[\alpha]_D$ = +57.3 (*c* 1.85, CH_2Cl_2); ^{1}H NMR (500 MHz, toluene-d_8, 70 °C, hydrogen atoms of Ph group omitted) δ: 4.43 (1H, d, *J* 12.0 Hz, OC*H*HPh), 4.13 (1H, d, *J* 12.0 Hz, OCH*H*Ph), 4.02 (1H, dd, *J* 10.5, 3.1 Hz, H_2), 3.86 (1H, dd, *J* 7.1, 6.0, 3.1 Hz, H_{1a}), 3.61 (1H, dd, *J* 10.5, 6.0 Hz, $H_{2'}$), 3.46 (1H, m, H_{4b}), 3.15–3.02 (2H, H_5, H_8), 2.99 (1H,m, H_{4a}), 2.44 (1H, m, $H_{8'}$), 1.76 (1H, m, H_6), 1.56 (1H, m, H_7), 1.05–0.85 (2H, $H_{6'}$, $H_{7'}$); ^{13}C NMR (125 MHz, toluene-d_8, carbon atoms of Ph group omitted): 175.3, 75.9, 74.5, 73.7, 70.7, 69.5, 51.9, 50.2, 20.9; IR (film) *v:* 1770 cm^{-1}; HR MS (ESI): *m/z* Calcd for [M+Na$^+$] $C_{16}H_{19}NO_4Na$: 312.1206. Found: 312.1200; Anal. Calcd for $C_{16}H_{19}NO_4$: C, 66.42; H, 6.62; N, 4.84. Found: C, 66.39; H, 6.60, N, 4.83; HPLC: LiChrospher Si60®, eluent: hexane/*i*-propanol 95:5, retention time 6.7 min.

4.2.2. (1*aS*,4*aR*,4*bS*,5*R*)-5-Benzyloxy-octahydrofuro[3,4-*d*]pyridin[1,2-*b*]isoxazol-4(*3H*)-one 32

Colourless oil, $[\alpha]_D^{25} = +11.3$ (*c* 0.6, CH_2Cl_2); ^{1}H NMR (500 MHz, toluene-d_8, hydrogen atoms of Ph group omitted) δ: 4.45 (1H, d, *J* 12.0 Hz, OC*H*HPh), 4.26 (1H, d, *J* 12.0 Hz, OCH*H*Ph), 4.05 (1H, ddd, *J* 7.7, 6.2, 2.1 Hz, H_{1a}), 3.98 (1H, dd, *J* 10.3, 2.1 Hz, H_2), 3.74 (1H, dd, *J* 10.3, 6.2 Hz, $H_{2'}$), 3.17 (1H, dd, *J* 10.3, 4.1 Hz, H_5), 3.10 (1H, m, H_8), 3.00 (1H, dd, *J* 7.7, 1.7 Hz, H_{4a}), 2.52 (1H, m, $H_{8'}$), 2.12 (1H, dd, *J* 10.3, 1.7 Hz, H_{4b}), 1.83 (1H, m, H_6), 1.58 (1H, m, H_7), 1.18 (1H, m, $H_{7'}$), 1.04 (1H, m, $H_{6'}$); ^{13}C NMR (125 MHz, toluene-d_8, carbon atoms of Ph group omitted): 174.2, 76.2, 75.2, 74.8, 73.9, 72.4, 54.8, 49.3, 30.7, 22.0; IR (film) *v:* 1767 cm^{-1}; HR MS (ESI): *m/z* Calcd for [M+Na$^+$] $C_{16}H_{19}NO_4Na$: 312.1206. Found: 312.1192; Anal. Calcd for $C_{16}H_{19}NO_4$: C, 66.42; H, 6.62; N, 4.84. Found: C, 66.38; H, 6.59; N, 4.84. HPLC: LiChrospher Si60®, eluent: hexane/*i*-propanol 95:5, retention time 11.8 min.

[‡] As we already demonstrated recently,[14b] the cycloaddition reactions between γ-lactones and five-membered nitrones are reversible and their stereochemical outcome depends on the reaction conditions. Such behavior has never been observed for the reactions involving δ-lactones regardless of the type of nitrone.[13] A reversibility of the reaction is also observed for the 1,3-DC of γ-lactones (**3**, **6**) with 6-membered nitrone **7**. The reflux of toluene solution of *exo-anti* adduct **31** gave, after 4 days, the equilibrium mixture of compounds **31** and **32** in the ratio 2:1.

4.2.3. (1*aR*,2*R*,4*aS*,4*bS*,5*R*)-5-Benzyloxy-2-hydroxymethyl-octahydrofuro[3,4-*d*]pyridino[1,2-*b*]isoxazol-4(3*H*)-one 33

Colourless oil; $[\alpha]_D$ = +2.2 (*c* 2.24, CH_2Cl_2); ^{1}H NMR (500 MHz, toluene-d_8, 90 °C, hydrogen atoms of Ph group omitted) δ: 4.41 (1H, d, *J* 12.0 Hz, OC*H*HPh), 4.20 (1H, d, *J* 12.0 Hz, OCH*H*Ph), 4.05 (1H, m, H_1), 3.99 (1H, m, H_2), 3.77–3.69 (2H, CH_2OH), 3.26 (1H, dd, *J* 12.0, 2.8 Hz, H_{4b}), 3.14–2.96 (3H, H_{4a}, H_5, H_8), 2.40 (1H, m, $H_{8'}$), 1.80 (1H, m, H_6), 1.52 (1H, m, H_7), 1.11–0.92 (2H, $H_{6'}$, $H_{7'}$); ^{13}C NMR (125 MHz, toluene-d_8, carbon atoms of Ph group omitted): 174.5, 82.8, 79.6, 76.3, 74.1, 72.0, 70.6, 63.3, 53.0, 49.7, 19.8; IR (film) *v*: 3433, 1769 cm^{-1}; HR MS (ESI): *m/z* Calcd for [M+Na$^+$] $C_{17}H_{21}NO_5Na$: 342.1312. Found: 342.1308; Anal. Calcd for $C_{17}H_{21}NO_5$: C, 63.94; H, 6.63; N, 4.39. Found: C, 63.95; H, 6.60; N, 4.36. HPLC: LiChrospher Si60®, eluent: hexane/*i*-propanol 90:10, retention time 9.3 min.

4.2.4. (1*aS*,2*R*,4*aR*,4*bS*,5*R*)-5-Benzyloxy-2-hydroxymethyl-octahydrofuro[3,4-*d*]pyridin[1,2-*b*]isoxazol-4(3*H*)-one (34)

Colourless oil; $[\alpha]_D$ = +100.3 (*c* 0.75, CH_2Cl_2); ^{1}H NMR (500 MHz, toluene-d_8, hydrogen atoms of Ph group omitted) δ: 4.75 (1H, d, *J* 11.0 Hz, OC*H*HPh), 4.54 (1H, d, *J* 11.0 Hz, OCH*H*Ph), 4.34 (1H, dd, *J* 7.5, 1.6 Hz, H_{1a}), 4.25 (1H, ddd, *J* 2.9, 2.7, 1.6 Hz, H_2), 3.70 (1H, m, H_5), 3.35 (1H, dd, *J* 7.5, 6.1 Hz, H_{4a}), 3.29 (1H, dd, *J* 12.1, 2.9 Hz, C*H*HOH), 3.21 (1H, m, H_8), 3.10 (1H, dd, *J* 12.1, 2.7 Hz, CH*H*OH), 2.20 (1H, dd, *J* 9.6, 6.1 Hz, H_{4b}), 2.12 (1H, m, $H_{8'}$), 1.80 (1H, m, H_6), 1.43–1.15 (2H, H_7), 0.90 (1H, m, $H_{6'}$); ^{13}C NMR (125 MHz, toluene-d_8, carbon atoms of Ph group omitted): 174.3, 86.6, 78.1, 74.9, 73.3, 71.9, 62.8, 54.4, 50.8, 30.3, 21.6; IR (film) *v*: 3436, 1767 cm^{-1}; HR MS (ESI): *m/z* Calcd for [M+Na$^+$] $C_{17}H_{21}NO_5$ Na: 342.1312. Found: 342.1305; Anal. Calcd for $C_{17}H_{21}NO_5$: C, 63.94; H, 6.63; N, 4.39. Found: C, 63.92; H, 6.62; N, 4.37. HPLC: LiChrospher Si60®, eluent: hexane/*i*-propanol 90:10, retention time 18.1 min.

4.3. The UV and CD measurements

The UV spectra were measured in acetonitrile on Varian Cary 100 spectrophotometer. The CD spectra were recorded between 180 and 360 nm at room temperature with a JASCO J-820 spectropolarimeter using acetonitrile solution. The solutions with concentration in the range of 0.5–1.0 × 10^{-4} mol/dm^3 were examined in cells with a path length of 0.1, 0.5 or 1 cm. For the solid-state CD measurements a sample of crystalline compound (1–3 mg) was ground with Nujol to form a homogenous Nujol mull, which was rotated around the optical axis during entire measurement using original JASCO equipment for this purpose. The low-temperature spectra were recorded in EPA (diethyl ether/*iso*-pentane/ethanol 5:5:2 v/v) solution with a concentration of 0.956 mmol/dm^3 in range of 210–350 nm in the 0.1- and 1-cm cells.

4.4. The computational methods

The quantum-mechanic calculations were carried out using GAUSSIAN 03 suite.[26] The geometry optimization of cycloadducts was carried out using DFT methods[17] at the B3LYP/6-31+G(d) level of theory.[28] The stationary points were characterized by the frequency calculations in order to verify that the obtained minima have zero imaginary frequency. The optimizations were carried out using Berny analytical gradient optimization method.[29]

The UV and CD spectra were simulated using time-dependent DFT (TD-DFT)[24] methods at the B3LYP/6-311+G(d,p) theory level. For the treatment of solvent effect, the polarized continuum model (PCM)[25] method was used with acetonitrile as the solvent.

The conformational search was carried out using HYPERCHEM v.7.5 suite program. For all molecular modelling calculations the MM+ force field method was used.[22]

Acknowledgement

We are most indebted to Mr. Grzegorz Lipner (IOC PAS, Warsaw) for providing us with computer capabilities.

References

1. (a) Padwa, A.. *1,3-Dipolar Cycloaddition Chemistry*; Wiley: New York, 1984; (b) Gothelf, K. V.; Jörgensen, K. A. *Chem. Rev.* **1998**, *98*, 863–909; (c) Karlsson, S.; Högberg, H.-E. *Org. Prep. Proced. Int.* **2001**, *33*, 103–172; (d) Kobayashi, S.; Jörgensen, K. A. *Cycloaddition Reactions in Organic Synthesis*; Wiley-VCH: Weinheim, 2002; (e) Pellissier, H. *Tetrahedron* **2007**, *63*, 3235–3285; (f) Padwa, A. In *Synthetic Applications of 1,3-Dipolar Cycloaddition Chemistry Toward Heterocycles and Natural Products*; Padwa, A., Pearson, W. H., Eds.; Wiley & Sons: Hoboken, NJ, 2003; (g) Merino, P.. In *Science of Synthesis*; Padwa, A., Ed.; George Thieme: New York, NY, 2004; Vol. 27, p 511.
2. (a) Gallos, J. K.; Koumbis, A. E. *Curr. Org. Chem.* **2003**, *7*, 397–426; (b) Gallos, J. K.; Koumbis, A. E. *Curr. Org. Chem.* **2003**, *7*, 771–797; (c) Koumbis, A. E.; Gallos, J. K. *Curr. Org. Chem.* **2003**, *7*, 585–628.
3. (a) Frederickson, M. *Tetrahedron* **1997**, *53*, 403–425; (b) Nair, V.; Suja, T. D. *Tetrahedron* **2007**, *63*, 12247–12275; (c) Broggini, G.; Zecchi, G. *Synthesis* **1999**, 905–917.
4. (a) Merino, P.; Tejero, T. *Molecules* **1999**, *4*, 169–179; (b) Revuelta, J.; Cicchi, S.; Goti, A.; Brandi, A. *Synthesis* **2007**, 485–504.
5. Ashry, E. S.; Nemr, A. *Synthesis of Naturally Occurring Nitrogen Heterocycles from Carbohydrates*; Blackwell Publishing: Oxford, 2005.
6. Hudlický, T.; Reed, J. W. *The Way of Synthesis*; Wiley-VCH: Weinheim, 2007.
7. Lopez, M. D.; Cobo, J.; Nogueras, M. *Curr. Org. Chem.* **2008**, *12*, 718–750.
8. (a) Cicchi, S.; Goti, A.; Brandi, A. *J. Org. Chem.* **1995**, *60*, 4743–4748; (b) Goti, A.; Cicchi, S.; Cacciarini, M.; Cardona, F.; Fedi, V.; Brandi, A. *Eur. J. Org. Chem.* **2000**, 3633–3645; (c) Cordero, F.; Pisaneschi, F.; Gensini, M.; Goti, A.; Brandi, A. *Eur. J. Org. Chem.* **2002**, 1941–1951; (d) Pisaneschi, F.; Cordero, F.; Brandi, A. *Eur. J. Org. Chem.* **2003**, 4373–7375; (e) Cardona, F.; Moreno, G.; Guarana, F.; Vogel, P.; Schetz, C.; Merino, P.; Goti, A. *J. Org. Chem.* **2005**, *70*, 6552–6555; (f) Pisaneschi, F.; Piacenti, M.; Cordero, F.; Brandi, A. *Tetrahedron: Asymmetry* **2006**, *17*, 292–296.
9. (a) Carmona, A. T.; Whigtman, R. H.; Robina, I.; Vogel, P. *Helv. Chim. Acta* **2003**, *86*, 3066–3073; (b) McCraig, A.; Meldrum, K. P.; Whigtman, R. H. *Tetrahedron* **1998**, *54*, 9429–9446; (c) Hull, A.; Meldrum, K. P.; Therand, P. R.; Whigtman, R. H. *Synlett* **1997**, 123–125; (d) McCraig, A.; Wightman, R. H. *Tetrahedron Lett.* **1993**, *34*, 3939–3941.
10. Kuban, J.; Kolarovic, A.; Fisera, L.; Jager, V.; Humpa, O.; Pronayova, N. *Synlett* **2001**, 1866–1868.
11. Tufariello, J. J. *J. Am. Chem. Soc.* **1980**, *102*, 373–376.
12. (a) Socha, D.; Jurczak, M.; Chmielewski, M. *Carbohydr. Res.* **2001**, *336*, 315–318; (b) Rabiczko, J.; Urbańczyk-Lipkowska, Z.; Chmielewski, M. *Tetrahedron* **2002**, *58*, 1433–1441; (c) Socha, D.; Paśniczek, K.; Jurczak, M.; Solecka, J.; Chmielewski, M. *Carbohydr. Res.* **2006**, *341*, 2005–2011; (d) Paśniczek, K.; Socha, D.; Solecka, J.; Jurczak, M.; Chmielewski, M. *Can. J. Chem.* **2006**, *84*, 534–539; (e) Panfil, I.; Solecka, J.; Chmielewski, M. *J. Carbohydr. Chem.* **2006**, *25*, 673–684; (f) Paśniczek, K.; Solecka, J.; Chmielewski, M. *J. Carbohydr. Chem.* **2007**, *26*, 195–211; (g) Stecko, S.; Jurczak, M.; Urbańczyk-Lipkowska, Z.; Solecka, J.; Chmielewski, M. *Carbohydr. Res.* **2008**, *343*, 2215–2220; (h) Stecko, S.; Solecka, J.; Chmielewski, M. *Carbohydr. Res.* **2009**, *344*, 167–176; (i) Stecko, S.; Paśniczek, K.; Jurczak, M.; Solecka, J.; Chmielewski, M. *Polish J. Chem.* **2009**, *83*, 237–243.
13. (a) Paśniczek, K.; Socha, D.; Jurczak, M.; Frelek, J.; Suszczyńska, A.; Urbańczyk-Lipkowska, Z.; Chmielewski, M. *J. Carbohydr. Chem.* **2003**, *22*, 613–629; (b) Socha, D.; Jurczak, M.; Frelek, J.; Klimek, A.; Rabiczko, J.; Urbańczyk-Lipkowska, Z.; Suwińska, K.; Chmielewski, M.; Cardona, F.; Goti, A.; Brandi, A. *Tetrahedron: Asymmetry* **2001**, *12*, 3163–3172; (c) Jurczak, M.; Rabiczko, J.; Socha, D.; Chmielewski, M.; Cardona, F.; Goti, A.; Brandi, A. *Tetrahedron: Asymmetry* **2000**, *11*, 2015–2022.
14. (a) Stecko, S.; Paśniczek, K.; Jurczak, M.; Urbańczyk-Lipkowska, Z.; Chmielewski, M. *Tetrahedron: Asymmetry* **2006**, *17*, 68–78; (b) Stecko, S.; Paśniczek, K.; Jurczak, M.; Urbańczyk-Lipkowska, Z.; Chmielewski, M. *Tetrahedron: Asymmetry* **2007**, *18*, 1085–1093.
15. (a) Stecko, S.; Paśniczek, K.; Michel, C.; Milet, A.; Perez, S.; Chmielewski, M. *Tetrahedron: Asymmetry* **2008**, *19*, 1660–1669; (b) Stecko, S.; Paśniczek, K.; Michel, C.; Milet, A.; Perez, S.; Chmielewski, M. *Tetrahedron: Asymmetry* **2008**, *19*, 2140–2148.
16. Legrand, M.; Bucourt, R. *Bull. Soc. Chim. Fr.* **1967**, 2241–2242.
17. Dreizler, R.; Gross, E. *Density Functional Theory*; Plenum Press: New York, 1995.
18. Crystallographic data for the structures **9**, **10**, **16**–**17** was reported before (see Ref. 14a,b) and are available from the Cambridge Crystallographic Data Center, Cambridge, UK, as a supplementary publications: **9** (CCDC No. 634391), **10** (CCDC No. 282893), **16** (CCDC No. 282892) and **17** (CCDC No. 282896). The crystallographic data for compound **15** were deposited in CCDC and are available as supplementary data (CCDC No. 722668).
19. Crystallographic data for the structures **22** and **25** was reported earlier (see Ref. 14a,b) and is available from the Cambridge Crystallographic Data Center, Cambridge, UK, as a Supplementary publications: **22** (CCDC No. 634282), **25** (CCDC No. 282895).

20. (a) Forzatto, C.; Nitti, P.; Pitacco, G.. *Tetrahedron: Asymmetry* **1997**, *8*, 4101–4110; (b) Forzatto, C.; Nitti, P.; Pitacco, G.; Valentin, E. *Tetrahedron: Asymmetry* **1999**, *10*, 1243–1254; (c) Castronovo, F.; Clericuzio, M.; Toma, L.; Vidari, G. *Tetrahedron* **2001**, *57*, 2791–2798.
21. Snatzke, G.; Snatzke, R. In *Analytiker-Taschenbuch Band 1*; Kienitz, H., Bock, R., Fresenius, W., Huber, W., Tölg, G., Eds.; Springer: Berlin, Heildelberg, New York,, 1980; pp 218–244.
22. (a) Allinger, N. L. *J. Am. Chem. Soc.* **1977**, *99*, 8127–8135; (b) N.L. Allinger, Y.H. Yuh, Quantum Chemistry Program Exchange, Bloomington, Indiana, Program No. 395, in: U. Burkert, N.L. Allinger (Eds.), Molecular Mechanics, ACS Monograph 177, American Chemical Society, Washington, D.C., 1982.; (c) Lii, J.; Gallion, S.; Bender, C.; Wikstrom, H.; Allinger, N. L.; Flurchick, K. M.; Teeter, M. M. *J. Comput. Chem.* **1989**, *10*, 503–512.
23. (a) Cid, P.; de March, P.; Figueredo, M.; Font, J.; Milan, S. *Tetrahedron Lett.* **1992**, *33*, 667–670; (b) Cid, P.; de March, P.; Figueredo, M.; Font, J.; Milan, S.; Soria, A.; Virgilli, A. *Tetrahedron* **1993**, *49*, 3857–3870; (c) Alonso-Perarnau, D.; de March, P.; Figueredo, M.; Font, J.; Soria, A. *Tetrahedron* **1993**, *49*, 4267–4274.
24. Autschbach, J.; Ziegler, T. *J. Chem. Phys.* **2002**, *116*, 891–896.
25. (a) Miertus, S.; Scrocco, E.; Tomasi, J. *J. Chem. Phys.* **1981**, *55*, 117–129; (b) Mennucci, B.; Tomasi, J. *J. Chem. Phys.* **1997**, *106*, 5151–5158.
26. Frisch, M. J.; Trucks, G. W.; Schlegel, H. B.; Scuseria, G. E.; Robb, M. A.; Cheeseman, J. R.; Montgomery, Jr., J. A.; Vreven, T.; Kudin, K. N.; Burant, J. C.; Millam, J. M.; Iyengar, S. S.; Tomasi, J.; Barone, V.; Mennucci, B.; Cossi, M.; Scalmani, G.; Rega, N.; Petersson, G. A.; Nakatsuji, H.; Hada, M.; Ehara, M.; Toyota, K.; Fukuda, R.; Hasegawa, J.; Ishida, M.; Nakajima, T.; Honda, Y.; Kitao, O.; Nakai, H.; Klene, M.; Li, X.; Knox, J. E.; Hratchian, H. P.; Cross, J. B.; Bakken, V.; Adamo, C.; Jaramillo, J.; Gomperts, R.; Stratmann, R. E.; Yazyev, O.; Austin, A. J.; Cammi, R.; Pomelli, C.; Ochterski, J. W.; Ayala, P. Y.; Morokuma, K.; Voth, G. A.; Salvador, P.; Dannenberg, J. J.; Zakrzewski, V. G.; Dapprich, S.; Daniels, A. D.; Strain, M. C.; Farkas, O.; Malick, D. K.; Rabuck, A. D.; Raghavachari, K.; Foresman, J. B.; Ortiz, J. V.; Cui, Q.; Baboul, A. G.; Clifford, S.; Cioslowski, J.; Stefanov, B. B.; Liu, G.; Liashenko, A.; Piskorz, P.; Komaromi, I.; Martin, R. L.; Fox, D. J. ; Keith, T.; Al-Laham, M. A.; Peng, C. Y.; Nanayakkara, A.; Challacombe, M.; Gill, P. M. W.; Johnson, B.; Chen, W.; Wong, M. W.; Gonzalez, C.; Pople, J. A. *GAUSSIAN 03, Revision B*.04; Gaussian, Inc.: Pittsburgh PA, 2003.
27. Ashoorzadeh, A.; Caprio, V. *Synlett* **2005**, 346–348.
28. (a) Becke, A. D. *J. Chem. Phys.* **1993**, *98*, 5648–5652; (b) Becke, A. D. *Phys. Rev. A* **1988**, *38*, 3098–3100; (c) Lee, C.; Yang, W.; Parr, R. G. *Phys. Rev. B* **1988**, *37*, 785–789.
29. Schlegel, H. B. Geometry Optimization on Potential Energy Surface. In *Modern Electronic Structure Theory;*; Yarkony, D. R., Ed.; World Scientific Publishing: Singapore, 1994.